Supporting Information for

GaN/MgI_2 van der Waals heterostructure: a two-factor tunable photocatalyst for hydrogen evolution

Hua Zhu[1], Yang Shen[1,*], Qianglong Fang[1], Xiaodong Yang[2,*],

Liang Chen[1,**], and Shiqing Xu[1]

[1] *Institute of Optoelectronics Technology, China Jiliang University, Hangzhou 310018, China*

[2] *Key Laboratory of Ecophysics and Department of Physics, Shihezi University, Xinjiang 832003, China*

***Corresponding authors:** Y. Shen (yshen@cjlu.edu.cn), X.D. Yang (yangxiaodong1209@hotmail.com) and L. Chen (lchen@cjlu.edu.cn).

S1. Convergence test of k-point mesh

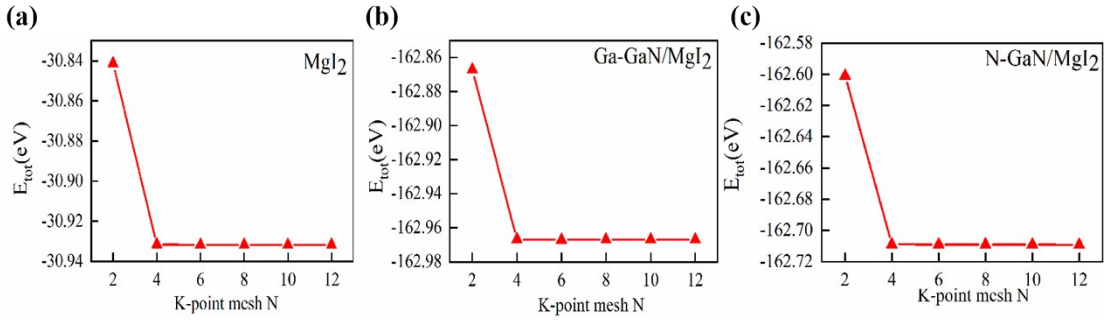

Figure S1. Total energies (E_{tot}) of (a) pristine MgI_2 monolayer, (b) MgI_2/Ga-GaN heterostructure, and (c) MgI_2/N-GaN heterostructure with different k-point mesh N (i.e., N×N×1).

S2. Band structures of hydrogenated GaN nanosheets

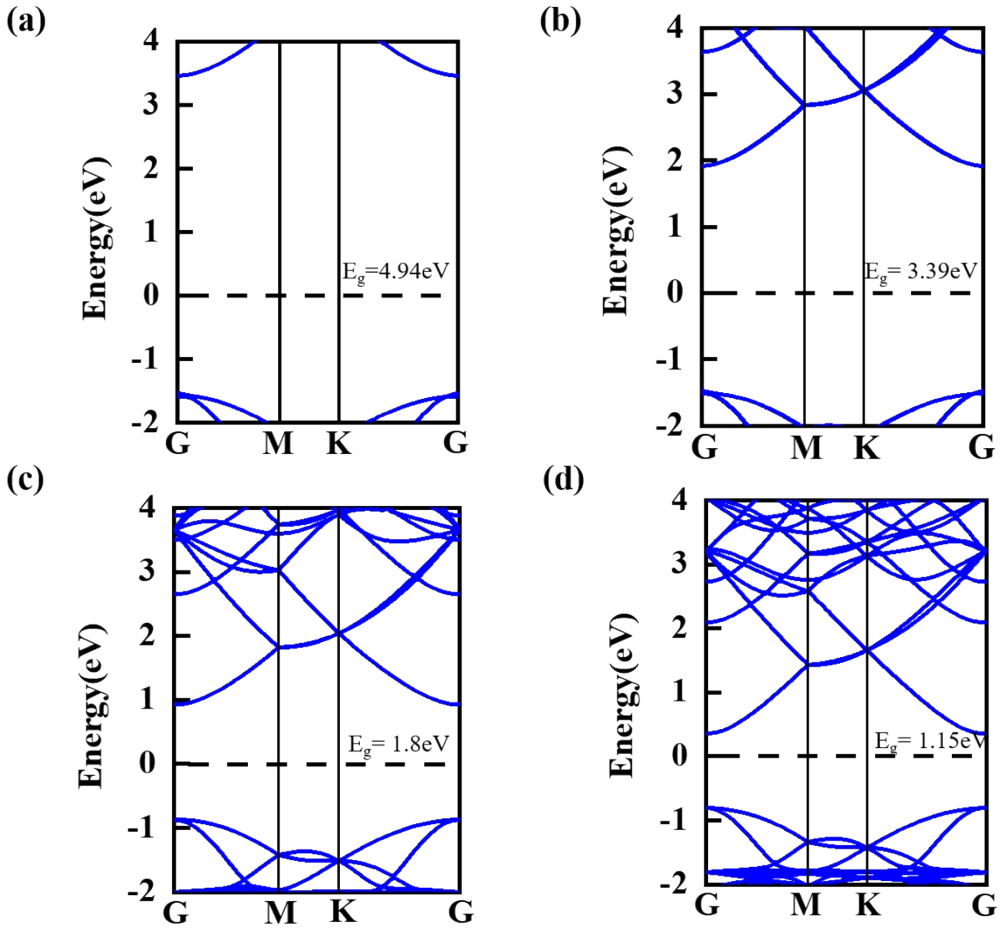

Figure S2. Band structure of (a) monolayer, (b) bilayer, (c) trilayer, and(d) tetralayer GaN nanosheets obtained using the HSE06 functional.

S3. the different stacking patten of GaN/MgI_2

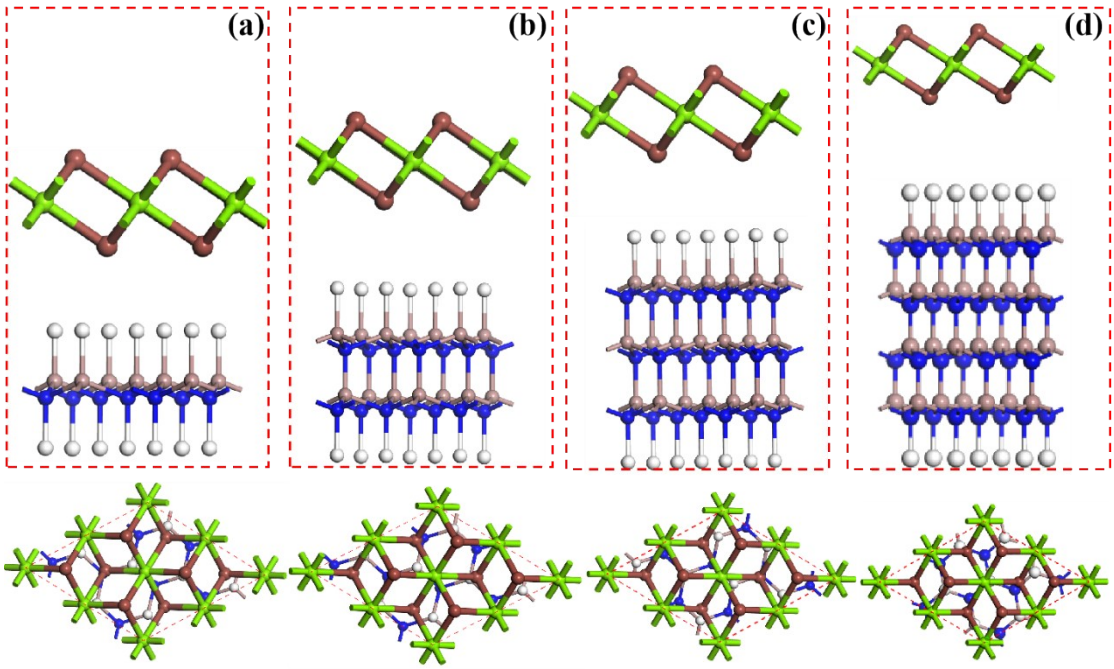

Figure S3. The different stacking patten of MgI_2/Ga-GaN heterostructures with the thickness of GaN layer in (a) monolayer, (b) bilayer, (c) trilayer and(d) tetralayer.

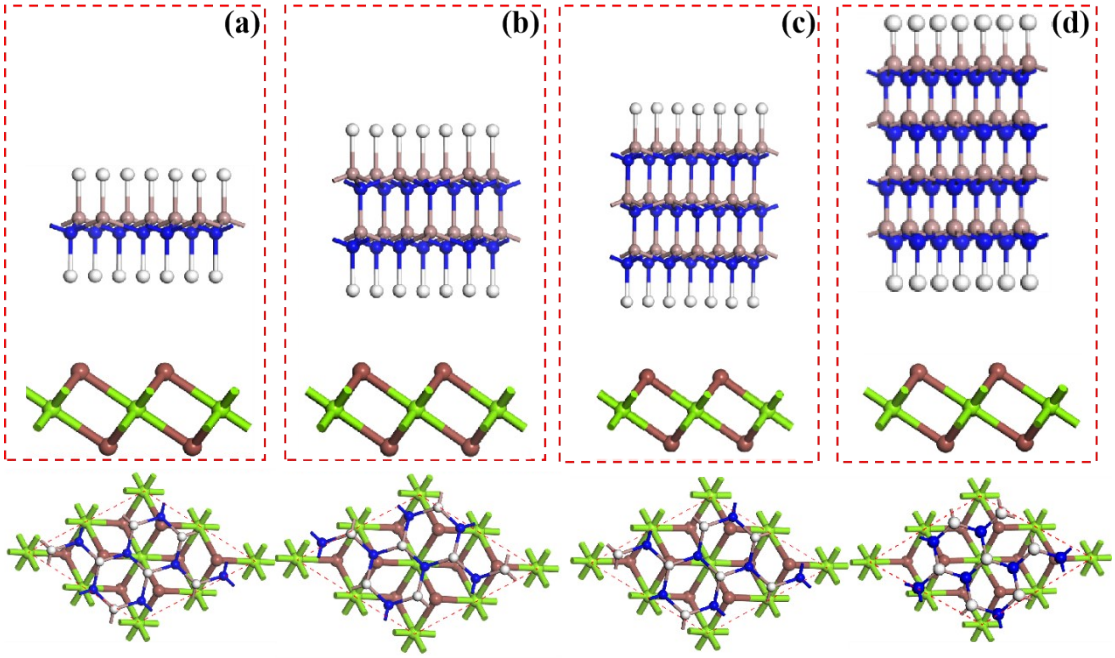

Figure S4. the different stacking patten of MgI_2/N-GaN heterostructures with the thickness of GaN layer in (a) monolayer, (b) bilayer, (c) trilayer and(d) tetralayer.

S4. Electrostatic potential distributions of 2D MgI_2/GaN heterostructures

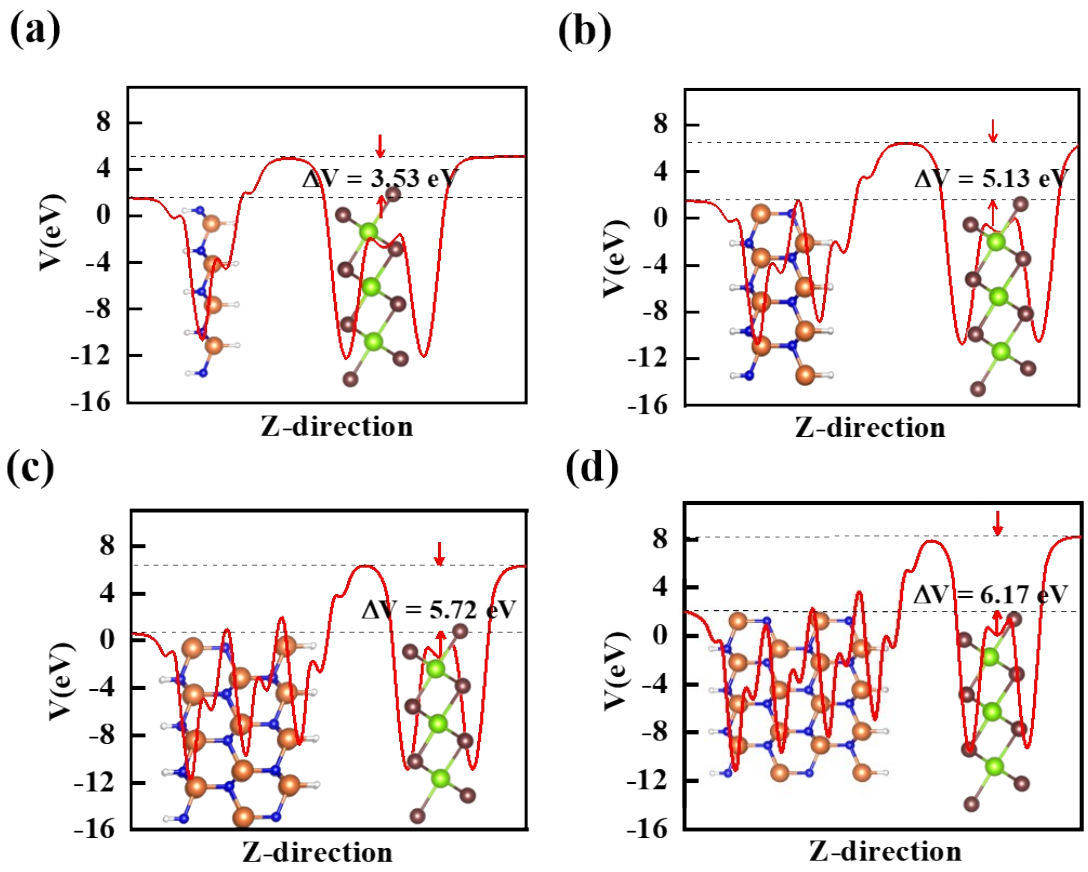

Figure S5. Electrostatic potential distribution (V) of MgI_2/Ga-GaN heterostructures with the thickness of GaN layer in (a) monolayer, (b) bilayer, (c) trilayer and(d) tetralayer. ΔV is the electrostatic potential difference between two terminations of the heterostructures.

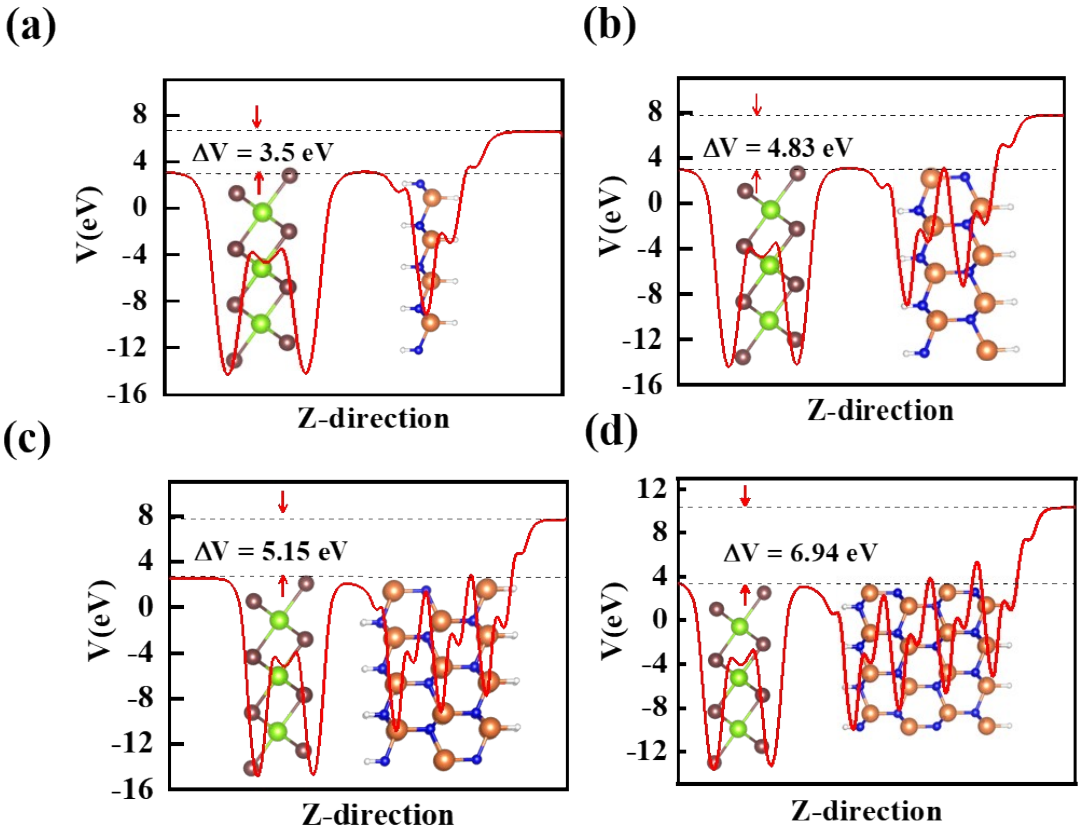

Figure S6. Electrostatic potential distribution (V) of MgI_2/N-GaN heterostructures with the thickness of GaN layer in (a) monolayer, (b) bilayer, (c) trilayer and(d) tetralayer. ΔV is the electrostatic potential difference between two terminations of the heterostructure.

S5. The charge-density isosurface distributions of CBM and VBM states of MgI_2/GaN heterostructures

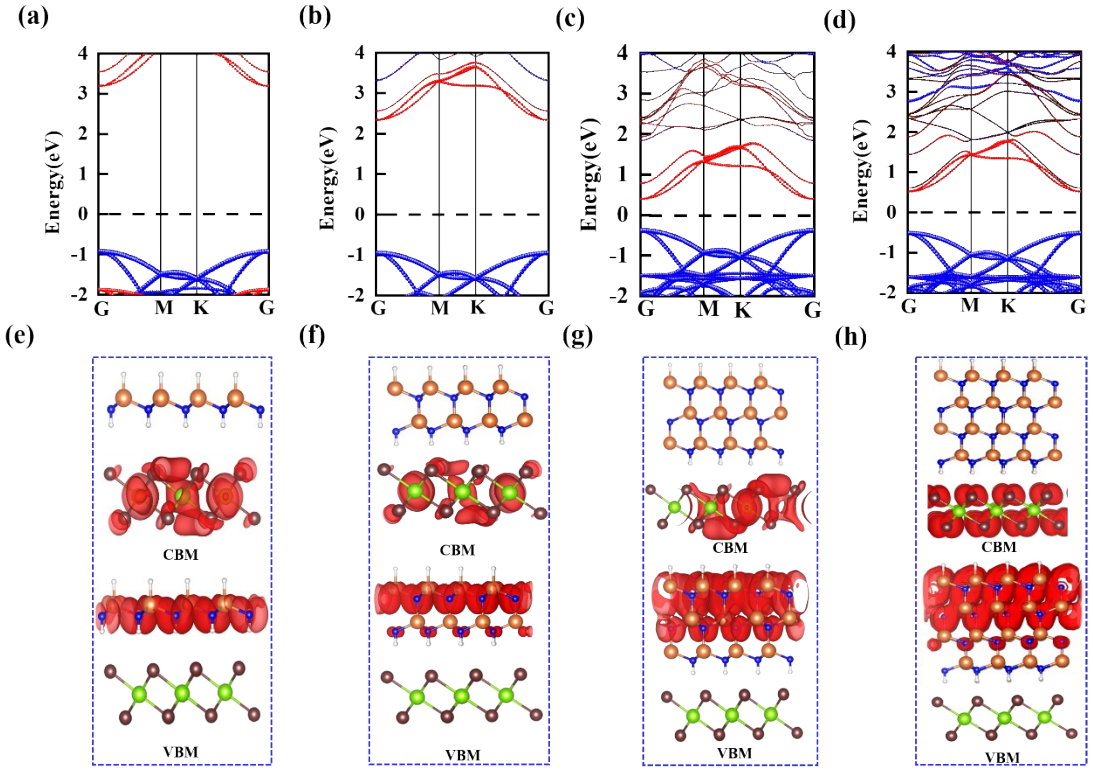

Figure S7. Projected band structure of N-GaN/MgI_2 heterostructures with the different GaN layers in (a) 1L, (b) 2L, (c) 3L, and (d) 4L. MgI_2 and GaN contributions to the heterostructures are represented by the red and blue balls, separately. The dashed lines indicate the Fermi level. CBM and VBM charge-density isosurfaces in 2D MgI_2/N-GaN heterostructures with GaN layer thickness in (e) 1L, (f) 2L, (g) 3L, and (h) 4L.

S6. Calculation of projected energy bands of deformed MgI_2-GaN heterojunctions by HSE method

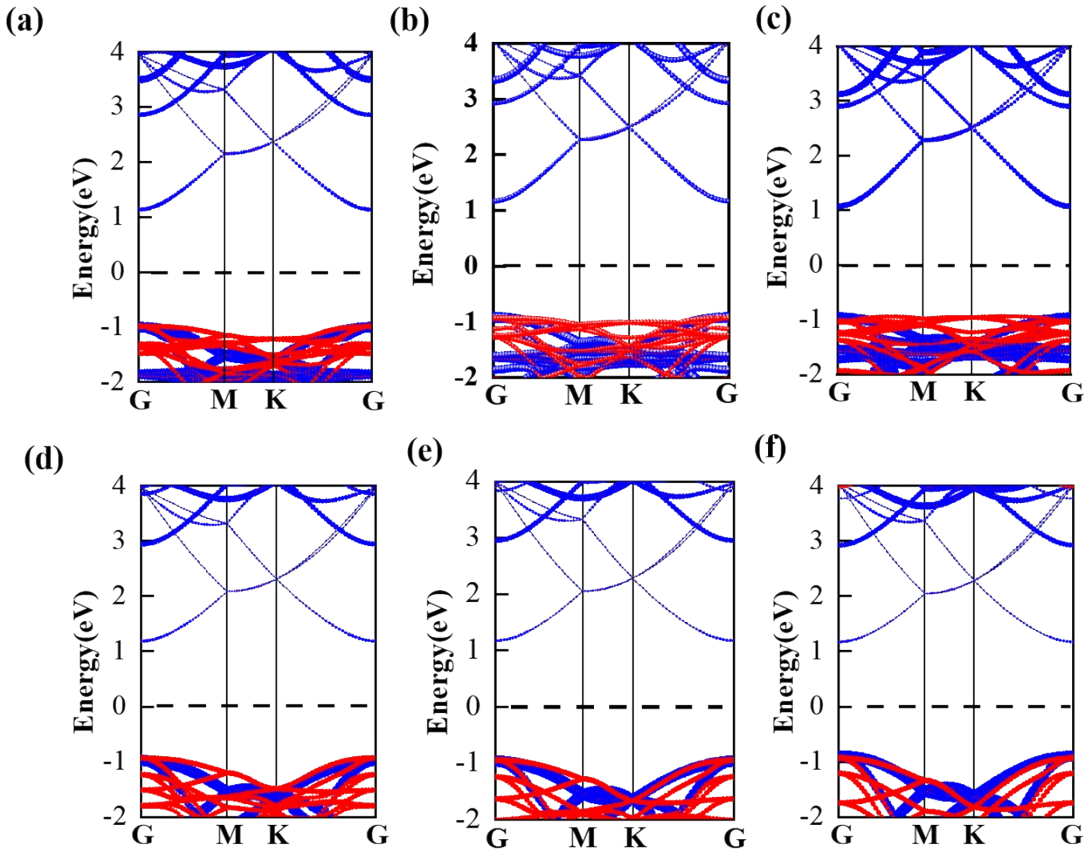

Figure S8. (a-c) Electronic band structures of 3L-Ga-GaN/MgI_2 under the effect of tensile strain, and(d-f) band structures due to compressive strain. Dashed black lines set to zero represent Fermi level.